MASSIVE DEGENERACY AND ANOMALOUS THERMODYNAMICS IN A HIGHLY FRUSTRATED ISING MODEL ON HONEYCOMB LATTICE

Milan Žukovič
Department of Theoretical Physics and Astrophysics, Institute of Physics
Faculty of Science
Pavol Jozef Šafárik University in Košice
Park Angelinum 9, 041 54 Košice, Slovak Republic
Email: milan.zukovic@upjs.sk

KEYWORDS

Frustrated spin model; Macroscopic degeneracy; Metropolis algorithm; Replica exchange Monte Carlo

ABSTRACT

We numerically study a prototypical frustrated Ising model on a honeycomb lattice with competing nearest- and second-nearest-neighbor antiferromagnetic interactions, J_1 and J_2, for the highly frustrated case of $J_1 = J_2$. We employ both standard (SMC) and a more sophisticated replica exchange (REMC) Monte Carlo simulations in effort to demonstrate the difficulties of using the former and advantages of using the latter approaches. The ground state of the system is highly degenerate and consists of frozen superantiferromagnetic (SAF) domains, separated by zero-energy domain walls (ZEDW), thus showing no conventional long-range ordering. We demonstrate that such states are difficult to access by using SMC due to complex multimodal energy landscape, characteristic for such systems. On the other hand, the REMC approach turns out to be more efficient in exploring it and thus reaching also states not accessible to SMC. At finite temperatures, the system shows a peculiar behavior with multiple anomalies in thermodynamic functions, which can be attributed to the transitions between several states with the SAF-like ordering characterized by different types of ZEDW.

INTRODUCTION

In the last decades frustrated spin models have been a hot topic in condensed matter physics (Diep and Koibuchi 2020). Frustration can be generated by the lattice geometry and/or by the competition between different kinds of interaction. It often results in highly degenerate ground states with new induced symmetries, which may give rise to unexpected and exotic behaviors at finite temperatures. In spite of intensive investigations, many properties of frustrated systems are still not very well understood. Their numerical simulations have turned out to be challenging and standard approaches, such as the Metropolis Monte Carlo (MC) simulation typically used in the study of classical spin systems, encountered many difficulties or completely failed. Typical problems result from the presence of complex multimodal free energy landscapes with local minima that are separated by entropic barriers. Conventional MC approaches suffer from long equilibration times due to the suppressed tunneling through these barriers or get trapped in metastable states. Overcoming large energy barriers at strong first-order phase transitions may be another problem.

Communications of the ECMS, Volume 36, Issue 1,
Proceedings, ©ECMS Ibrahim A. Hameed, Agus Hasan,
Saleh Abdel-Afou Alaliyat (Editors) 2022
ISBN: 978-3-937436-77-7/978-3-937436-76-0(CD) ISSN 2522-2414

Ising models on bipartite lattices with further-neighbor antiferromagnetic (AF) interactions are paradigmatic examples of the spin systems frustrated due to the interaction competition. In the most studied two-dimensional Ising antiferromagnet on a square lattice the competition between the nearest-neighbor interaction J_1 (ferromagnetic or antiferromagnetic) and the increasing AF second-nearest-neighbor interaction J_2 leads to a gradual increase of frustration, which is reflected in reduction of the critical temperature down to zero at $R \equiv J_2/|J_1| = -1/2$ (Landau 1980; Grynberg and Tanatar 1992; Morán-López et al. 1993; Moran-Lopez et al. 1994). A possible change of the transition to the first order near $R = -1/2$ has also been reported (Jin et al. 2013; Bobák et al. 2015). For $R < -1/2$ the system shows a phase transition to a peculiar striped or superantiferromagnetic (SAF) state with a lot of controversy regarding its character. A series of earlier studies predicted a second-order transition with non-universal critical exponents for any $R < -1/2$ (see Malakis et al. (2006) and references within), however, some more recent approaches favored a first-order transition for $R^* < R < -1/2$ and a second-order one only for $R < R^*$ (Morán-López et al. 1993; Moran-Lopez et al. 1994; dos Anjos et al. 2008; Kalz et al. 2008, 2011; Jin et al. 2012; Bobák et al. 2015). The value of R^* was in different studies estimated to range between -1.1 (Morán-López et al. 1993) and -0.67 (Jin et al. 2012).

Much less attention has been devoted to the frustrated $J_1 - J_2$ model on other bipartite lattices, albeit, their critical behavior might be quite different from the square lattice one. In the present study we focus on the $J_1 - J_2$ Ising model on a honeycomb lattice, in which the small coordination number together with frustrated interactions has been shown to have interesting effects in the Heisenberg model with a magnetically disordered region and a spin-liquid phase (Zhang and Lamas 2013; Cabra et al. 2011). This frustrated model is also interesting from the experimental point of view, since it can be applied to some real materials (Matsuda et al. 2010; Tsirlin et al. 2010). The ground state of the $J_1 - J_2$ Ising model was investigated in some earlier papers (Houtappel 1950; Kudō and Katsura 1976; Katsura et al. 1986) but its critical behavior was studied only recently by the effective field theory (EFT) (Bobák et al. 2016), the MC simulation (Žukovič et al. 2020; Žukovič 2021), cluster mean-field (CMF) (Schmidt and Godoy 2021) and machine learning (ML) (Corte et al. 2021; Acevedo et al. 2021) approaches. For smaller degree of frustration, namely within the interval $-1/4 < R < 0$, the critical behavior resembles that for the square lattice. In particular, with the increasing frustration

due to increasing $|J_2|$ the transition temperature gradually decreases down to zero at $R = -1/4$. A possible crossover to the first-order behavior was suggested by the EFT (Bobák et al. 2016) but not confirmed by either MC (Žukovič 2021) or CMF (Schmidt and Godoy 2021).

In the present study we focus on the highly frustrated region of $R < -1/4$, for which both the EFT and CMF analytical approximations predicted no phase transition but the numerical approaches indicated some kind of phase transition to a highly degenerate low-temperature phase with no long-range ordering (Žukovič et al. 2020; Corte et al. 2021; Acevedo et al. 2021). In our previous study, focused on the less frustrated case of $-1/4 < R < 0$, we demonstrated that with the increasing frustration ($R \to -1/4$ and $T \to 0$) the system tends to freeze in metastable domain states separated by large energy barriers with extremely sluggish dynamics. In such cases the standard MC simulations turn out to be either very inefficient or completely failing in reaching the stable thermal equilibrium state and that the tunneling through the energy barriers can be considerably improved by using the replica exchange MC approach (Žukovič 2021). Therefore, to better handle the above mentioned problems, here we employ the replica exchange MC method and confront the obtained results with those from the standard MC simulation.

MODEL AND METHODS

Model

We study the Ising model on the honeycomb lattice described by the Hamiltonian

$$\mathscr{H} = -J_1 \sum_{\langle i,j \rangle} s_i s_j - J_2 \sum_{\langle i,k \rangle} s_i s_k, \tag{1}$$

where $s_i = \pm 1$ is the Ising spin variable at the ith site and the summations $\langle i,j \rangle$ and $\langle i,k \rangle$ run over all nearest and second-nearest spin pairs, respectively. The competition between the nearest- and second-nearest neighbor AF interactions ($J_1 < 0$ and $J_2 < 0$) leads to frustration. In the following we restrict our considerations to the case of $J_1 = J_2$, i.e., $R = -1$.

Methods

Standard Monte Carlo (SMC): We consider the system sizes $L \times L$, with $L = 12 - 72$, and apply periodic boundary conditions. We note that the presence of high frustration restricts our considerations to relatively small values of L since the above mentioned difficulties escalate very quickly as the system size increases. In the SMC simulations we employ a vectorized (checkerboard) single-spin flip Metropolis algorithm. For thermal averaging of the calculated quantities at each value of the temperature T we perform from 10^5 up to 10^6 MC sweeps (MCS) after discarding the initial burn-in period corresponding to twenty percent of those numbers for thermalization. Due to the low-temperature freezing of the system in metastable states in our simulations we use both cooling and heating protocols. Namely, the simulations are initialized from random (SAF) state at high (low) temperatures and then proceed towards lower (higher) temperatures with the step $k_B \Delta T/|J_1| = -0.01$ (0.01). The next simulation starts from the final configuration obtained at the previous temperature to keep the system close to the equilibrium during the entire simulation.

Replica exchange Carlo (REMC): In effort to alleviate the difficulties of the standard MC approach we apply the REMC or parallel tempering method (Hukushima and Nemoto 1996), which is designed to more efficiently overcome energy barriers by a random walk in temperature space and allows better exploration of complex energy landscapes. Using the REMC method, we run simulations at $N_T = 120$ temperatures (replicas) in parallel and propose 10^5 swaps between replicas followed by 100 MCS over the complete lattice. The swap acceptance rate between neighboring replicas is $P(\beta_i \leftrightarrow \beta_{i+1}) = \min\{1, \exp(\Delta\beta\Delta\mathscr{H})\}$, where $\Delta\beta = \beta_{i+1} - \beta_i$ and $\Delta\mathscr{H} = \mathscr{H}_{i+1} - \mathscr{H}_i$ are differences between the neighboring inverse temperatures, $\beta_i = |J_1|/k_B T_i$, and the energies of the corresponding configurations, respectively. The temperatures T_i are chosen with the focus on the simulation bottlenecks in the vicinity of the expected transition temperatures to ensure sufficient acceptance rates (approximately flat) within the whole temperature interval.

The calculated quantities are restricted to the internal energy per spin $e \equiv E/N|J_1| = \langle \mathscr{H} \rangle / N|J_1|$, where $N = L^2$ is the number of spins, and the specific heat per spin obtained as

$$C/N = \frac{\langle \mathscr{H}^2 \rangle - \langle \mathscr{H} \rangle^2}{NT^2}, \tag{2}$$

where $\langle \cdots \rangle$ denotes the thermal average. The peaks in the latter quantity are useful for capturing various anomalies and/or phase transitions.

RESULTS

In the regime of $R < -1/4$ the ground state (GS) corresponds to a spin arrangement with the energy $E_{SAF}/N|J_1| = -1/2 + R$ (Kudō and Katsura 1976; Katsura et al. 1986; Bobák et al. 2016). Such energy is realized in any spin configuration with the following local arrangement: out of the three nearest-neighbor bonds two are antiferromagnetic and one ferromagnetic and out of the six second-nearest-neighbor bonds four are antiferromagnetic and two ferromagnetic. However, there are many lattice spin configurations (see Fig. 1 for two examples) fulfilling these constraints. This leads to macroscopic degeneracy and the absence of any long-range ordering in the system.

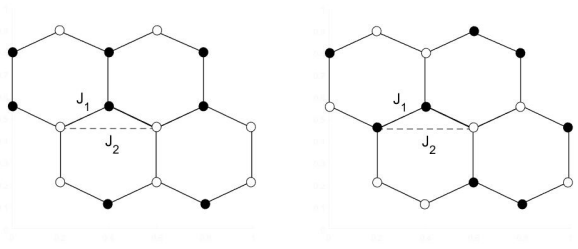

(a)SAF ordering #1 (b)SAF ordering #2

Fig. 1. Ground state for $R < -1/4$: Two examples of possible SAF ordering. The empty and filled circles represent spin-up and spin-down states, and the solid and dashed lines represent the interactions J_1 and J_2.

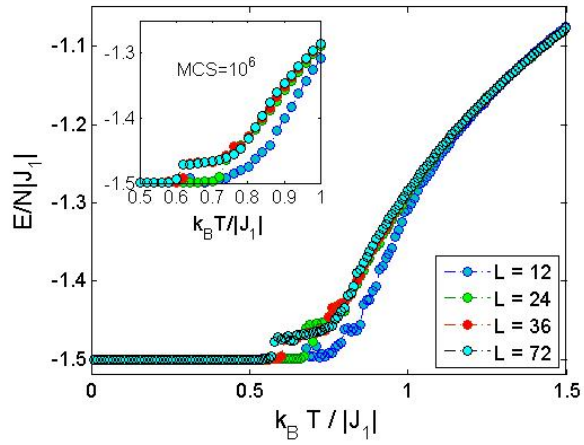

(a)Internal energy (SMC)

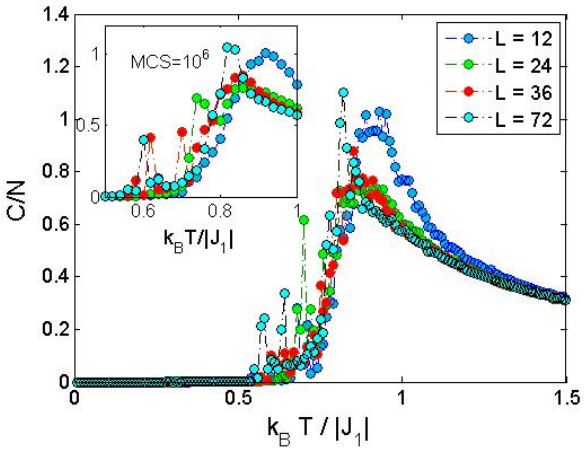

(b)Specific heat (SMC)

Fig. 2. Temperature dependencies of (a) the internal energy and (b) the specific heat for different lattice sizes L and 10^5 MCS, obtained from SMC. The insets show the results for 10^6 MCS.

Fig. 2 shows temperature variations of the internal energy and the specific heat obtained from the shorter runs (10^5 MCS) using SMC. For the smallest lattice size the internal energy curve shows at $k_BT/|J_1| \approx 0.9$ an anomaly characteristic for a continuous phase transition reflected in a specific heat peak (Fig. 2(b)). However, for larger L another anomaly appears at lower temperatures as a discontinuous decrease in the internal energy and the specific heat showing a spike-like peak at $k_BT/|J_1| \approx 0.6$, suggesting a first-order phase transition. The insets demonstrate that these features also persist in much longer runs (10^6 MCS). Just below this jump of the internal energy thermal fluctuations are strongly suppressed and the system freezes in a state corresponding to the expected GS energy of $E_{SAF}/N|J_1| = -3/2$.

To better understand this unconventional behavior we performed several independent SMC runs for the largest lattice size, $L = 72$, following the temperature-decreasing as well as temperature-increasing processes. The former are initialized at high temperatures by random configurations and the latter start at low temperatures from the SAF states. We can see a relatively large variability in the calculated quantities corresponding to the individual runs. An example showing the temperature variations of the energy for two runs of each

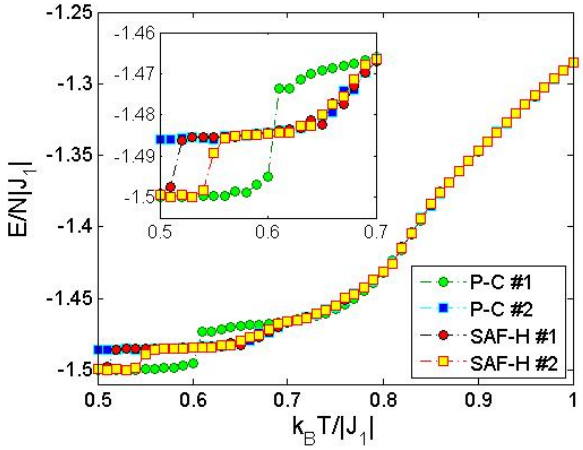

Fig. 3. Temperature dependencies of the internal energy for $L = 72$ and 10^6 MCS, obtained from SMC for two independent replicas cooled from paramagnetic phase (P-C #1,2) and two others heated from SAF phase (SAF-H #1,2).

kind are presented in Fig. 3. One can see that in the cooling process one simulation (green circles) lead to the low-temperature states with the energies close to the GS value, while the other one (blue squares), after some decrease below $k_BT/|J_1| \approx 0.7$ got stuck in a metastable state with the energy larger than the GS one. On the other hand, in the heating process all the runs start from the (SAF) configurations corresponding to the GS energy $E_{SAF}/N|J_1| = -3/2$. At some point of the heating the energies show a discontinuous increase but the temperatures at which this jump occurs in different runs are different (see red circles and yellow squares). At higher temperatures there are some additional smaller anomalies in the energy curves. This peculiar behavior signals the presence of metastable states corresponding to local minima in the rugged energy landscape.

To secure thermal equilibrium states we subsequently applied REMC simulations. The internal energy and the specific heat temperature variations for different lattice sizes are presented in Fig. 4. Compared to the similar dependencies obtained from SMC, shown in Fig. 2, the REMC curves are smoother and all the energy curves reached the values close to the GS value at all temperatures below $k_BT/|J_1| \approx 0.4$. Nevertheless, the anomalies observed in the SMC simulations are reproduced also in the REMC runs. In particular interesting is their lattice size dependence. As L increases the number of anomalies in both the energy and specific heat curves also increases, starting from two for $L = 24$ (or one for $L = 12$ not shown here) up to four for $L = 74$. The new ones keep forming at gradually lower temperatures creating wave-like dependencies.

Furthermore, the character of the lower-temperature anomalies resembles that observed at the first-order phase transitions. This is demonstrated in Fig. 5(a) by showing in the insets a bimodal character of the energy histograms at the temperatures corresponding to two low-temperature anomalies for the largest system size. On the other hand, the highest-temperature anomaly in the energy curve remains smooth but the corresponding specific heat peak increases with the lattice size like at a phase transition (see Fig. 5(b)).

Finally, let us inspect the character of the phases in the

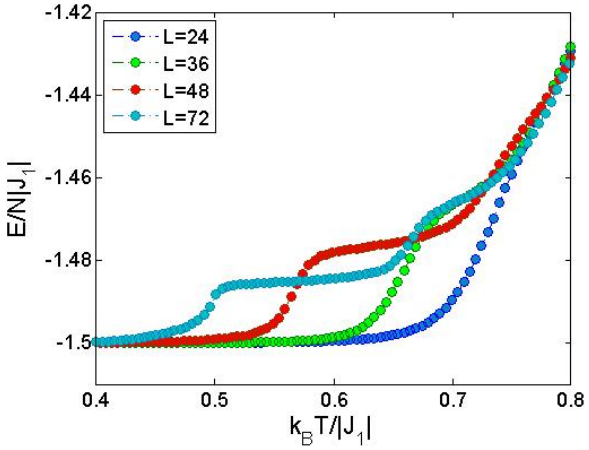

(a)Internal energy (REMC)

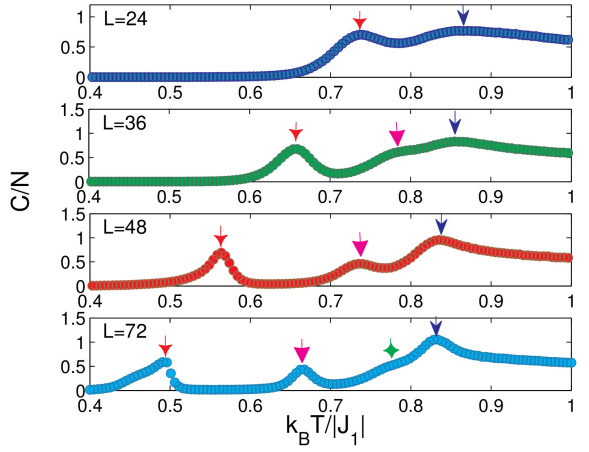

(b)Specific heat (REMC)

Fig. 4. Temperature dependencies of (a) the internal energy and (b) the specific heat for different lattice sizes L, obtained from REMC. Different arrows in (b) show the positions of the respective anomalies.

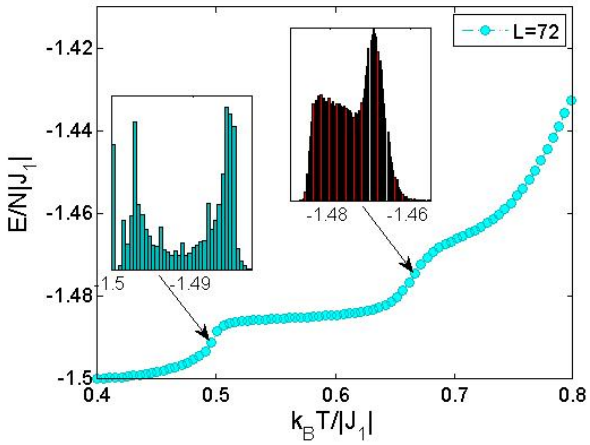

(a)Internal energy (REMC)

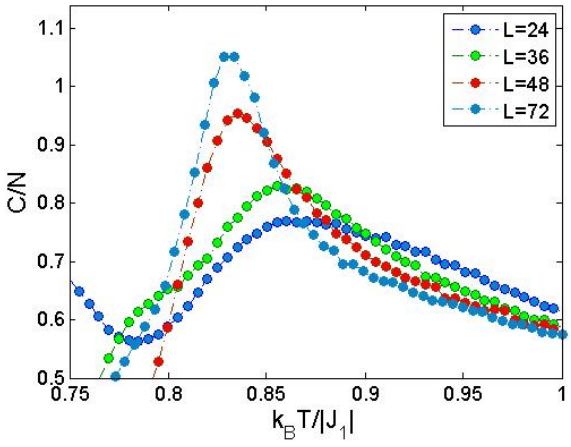

(b)Specific heat (REMC)

Fig. 5. Temperature dependencies of (a) the internal energy at lower temperatures and $L = 72$ and (b) the specific heat at higher temperatures and different L. The insets in (a) show the energy histograms at the temperatures corresponding to the anomalies.

temperature ranges between different anomalies. In Fig. 6 we show some typical spin configurations at different temperatures from REMC simulations for $L = 72$. The empty and filled circles represent spin-up and spin-down states, respectively. At the lowest temperature, $k_BT/|J_1| = 0.4$, one can notice that there is no long-range ordering that would span the entire lattice. Instead, the lattice is split into several domains with different types of SAF ordering inside each domain. The respective domains form horizontal bands of different widths and are separated from each other by zero-energy domain walls (ZEDW) spanning the entire lattice in the horizontal direction. At higher temperature, $k_BT/|J_1| = 0.57$, which falls within the temperature range between the two low-temperature anomalies, the spin texture is somewhat different. The lattice is still spit into several domains with SAF ordering, which are separated by ZEDW, however, the domain wall direction is now diagonal. One can also notice some isolated defects, which deform the boundary shape and increase the domain wall energy (empty and filled circles with magenta and cyan edges). We believe that these defects result from the increased thermal fluctuations which partially disrupt the perfect SAF-like ordering and slightly increase the energy. At still higher temperature, $k_BT/|J_1| = 0.72$, above the second low-temperature anomaly, there is still SAF-type of ordering fragmented in multiple domains with ZEDW. Here, however, the domains are smaller and do not necessarily span the entire system. Consequently, there is a mixture of shorter horizontal and vertical domain walls as illustrated in Fig. 6(c) by highlighting just a few of them. At the elevated temperature, naturally, there is also higher occurrence of defects due to thermal fluctuations.

CONCLUSIONS

We studied the frustrated Ising model model on a honeycomb lattice with competing nearest- and second-nearest-neighbor AF interactions, J_1 and J_2, in the highly frustrated region of $R \equiv J_2/|J_1| < -1/4$. We employed both SMC and REMC simulations in effort to demonstrate the difficulties of using the former and advantages of using the latter approaches in a numerical study of such a paradigmatic example of frustrated spin systems. We showed that the ground state of the system is highly degenerate and consists of frozen SAF-like domains, separated by zero-energy domain walls (ZEDW), with no conventional magnetic long-

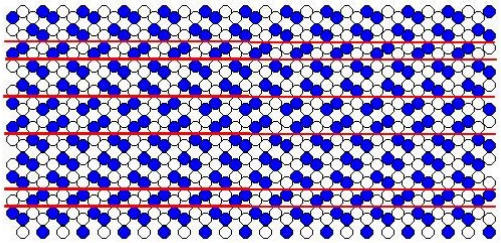

(a)$k_BT/|J_1| = 0.4$

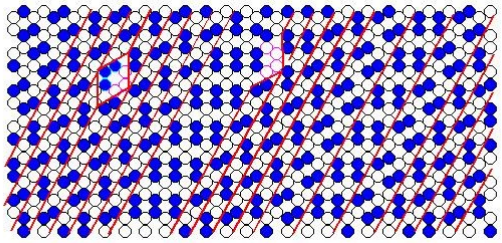

(b)$k_BT/|J_1| = 0.57$

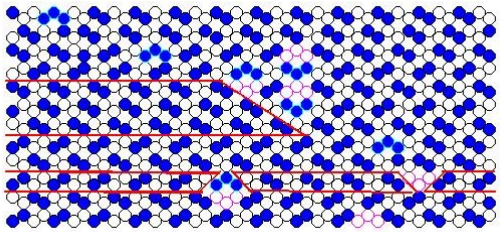

(c)$k_BT/|J_1| = 0.72$

Fig. 6. Typical spin snapshots at different temperatures from REMC simulations for $L = 72$. The empty (filled) circles represent spins up (down) and (a) the horizontal, (b) the diagonal and (c) the horizontal and diagonal red lines mark SAF domain walls. The empty and filled circles with magenta and cyan edges in (b) and (c) mark defects in perfect SAF-like ordering.

range ordering. We also demonstrated that such a state might be difficult to access by using the SMC, which might get stuck in metastable states. On the other hand, the REMC approach can more efficiently explore complex energy landscapes, characteristic for such systems, and thus reach also states not accessible to the SMC.

At finite temperatures, the system displayed a peculiar behavior with multiple anomalies in thermodynamic functions. The anomalies can be attributed to the transitions between several states with the SAF-like ordering, characterized by different types of ZEDW. The low-temperature anomalies bear some features of the first-order phase transitions, nevertheless, their number and positions show strong finite-size effects. Therefore, in order to verify whether the observed anomalies are just finite-size artifacts or at least some of them signal true phase transitions, a careful finite-size scaling analysis involving much larger system sizes to inspect the approach to the thermodynamic limit would be desirable. This goal might be achievable by implementing the REMC approach on the highly parallel GPU architecture, since the GPU-accelerated MC simulations of spin systems have been reported to achieve speedups up to three orders of magnitude compared to the standard CPU implementations (Weigel 2012).

ACKNOWLEDGMENTS

This work was supported by the grants of the Slovak Research and Development Agency (Grant No. APVV-18-0197) and the Scientific Grant Agency of Ministry of Education of Slovak Republic (Grant No. 1/0531/19).

REFERENCES

Acevedo, S., Arlego, M., and Lamas, C. A. (2021). Phase diagram study of a two-dimensional frustrated antiferromagnet via unsupervised machine learning. *Physical Review B*, 103(13):134422.

Bobák, A., Lučivjanskỳ, T., Borovskỳ, M., and Žukovič, M. (2015). Phase transitions in a frustrated ising antiferromagnet on a square lattice. *Physical Review E*, 91(3):032145.

Bobák, A., Lučivjanskỳ, T., Žukovič, M., Borovskỳ, M., and Balcerzak, T. (2016). Tricritical behaviour of the frustrated ising antiferromagnet on the honeycomb lattice. *Physics Letters A*, 380(34):2693–2697.

Cabra, D. C., Lamas, C. A., and Rosales, H. D. (2011). Quantum disordered phase on the frustrated honeycomb lattice. *Physical Review B*, 83(9):094506.

Corte, I., Acevedo, S., Arlego, M., and Lamas, C. (2021). Exploring neural network training strategies to determine phase transitions in frustrated magnetic models. *Computational Materials Science*, 198:110702.

Diep, H. T. and Koibuchi, H. (2020). Frustrated magnetic thin films: Spin waves and skyrmions. In *Frustrated Spin Systems: 3rd Edition*, pages 631–719. World Scientific.

dos Anjos, R. A., Viana, J. R., and de Sousa, J. R. (2008). Phase diagram of the ising antiferromagnet with nearest-neighbor and next-nearest-neighbor interactions on a square lattice. *Physics Letters A*, 372(8):1180–1184.

Grynberg, M. D. and Tanatar, B. (1992). Square ising model with second-neighbor interactions and the ising chain in a transverse field. *Physical Review B*, 45(6):2876.

Houtappel, R. M. F. (1950). Order-disorder in hexagonal lattices. *Physica*, 16(5):425–455.

Hukushima, K. and Nemoto, K. (1996). Exchange monte carlo method and application to spin glass simulations. *Journal of the Physical Society of Japan*, 65(6):1604–1608.

Jin, S., Sen, A., Guo, W., and Sandvik, A. W. (2013). Phase transitions in the frustrated ising model on the square lattice. *Physical Review B*, 87(14):144406.

Jin, S., Sen, A., and Sandvik, A. W. (2012). Ashkin-teller criticality and pseudo-first-order behavior in a frustrated ising model on the square lattice. *Physical Review Letters*, 108(4):045702.

Kalz, A., Honecker, A., Fuchs, S., and Pruschke, T. (2008). Phase diagram of the ising square lattice with competing interactions. *The European Physical Journal B*, 65(4):533–537.

Kalz, A., Honecker, A., and Moliner, M. (2011). Analysis of the phase transition for the ising model on the frustrated square lattice. *Physical Review B*, 84(17):174407.

Katsura, S., Ide, T., and Morita, T. (1986). The ground states of the classical heisenberg and planar models on the triangular and plane hexagonal lattices. *Journal of statistical physics*, 42(3):381–404.

Kudō, T. and Katsura, S. (1976). A method of determining the orderings of the ising model with several neighbor interactions under the magnetic field and applications to hexagonal lattices. *Progress of Theoretical Physics*, 56(2):435–449.

Landau, D. (1980). Phase transitions in the ising square lattice with next-nearest-neighbor interactions. *Physical Review B*, 21(3):1285.

Malakis, A., Kalozoumis, P., and Tyraskis, N. (2006). Monte carlo studies of the square ising model with next-nearest-neighbor interactions. *The European Physical Journal B-Condensed Matter and Complex Systems*, 50(1):63–67.

Matsuda, M., Azuma, M., Tokunaga, M., Shimakawa, Y., and Kumada, N. (2010). Disordered ground state and magnetic field-induced long-range order in an s= 3/2 antiferromagnetic honeycomb lattice compound bi 3 mn 4 o 12 (no 3). *Physical review letters*, 105(18):187201.

Morán-López, J., Aguilera-Granja, F., and Sanchez, J. (1993). First-order phase transitions in the ising square lattice with first-and second-neighbor interactions. *Physical Review B*, 48(5):3519.

Moran-Lopez, J., Aguilera-Granja, F., and Sanchez, J. (1994). Phase transitions in ising square antiferromagnets with first-and second-neighbour interactions. *Journal of Physics: Condensed Matter*, 6(45):9759.

Schmidt, M. and Godoy, P. (2021). Phase transitions in the ising antifer-

romagnet on the frustrated honeycomb lattice. *Journal of Magnetism and Magnetic Materials*, 537:168151.

Tsirlin, A. A., Janson, O., and Rosner, H. (2010). β-cu 2 v 2 o 7: A spin-1 2 honeycomb lattice system. *Physical Review B*, 82(14):144416.

Weigel, M. (2012). Performance potential for simulating spin models on gpu. *Journal of Computational Physics*, 231(8):3064–3082.

Zhang, H. and Lamas, C. A. (2013). Exotic disordered phases in the quantum j 1-j 2 model on the honeycomb lattice. *Physical Review B*, 87(2):024415.

Žukovič, M. (2021). Critical properties of the frustrated ising model on a honeycomb lattice: A monte carlo study. *Physics Letters A*, 404:127405.

Žukovič, M., Borovský, M., Bobák, A., Balcerzak, T., and Szałowski, K. (2020). Spin-glass-like ordering in a frustrated j 1-j 2 ising antiferromagnet on a honeycomb lattice. *Acta Physica Polonica, A.*, 137(5).

MILAN ŽUKOVIČ was born in Svidník, Slovakia and obtained his PhD degree in applied physics from Kyushu University, Japan in 2000. He pursued his research in the field of theoretical condensed matter physics at Kyushu University for two more years, before he assumed a position in automotive industry within Yazaki Corporation. In 2006-2008, he was involved in the research in modeling of spatial random fields as a Marie-Curie postdoc at Technical University of Crete, Greece. Since 2009 he has been with the Institute of Physics, Pavol Jozef Šafárik University in Košice, Slovakia, currently as a Professor of Physics. His e-mail address is: `milan.zukovic@upjs.sk` and his Webpage can be found at: `https://ufv.science.upjs.sk/zukovic/`.